

# Data-Driven Affinely Adjustable Robust Volt/VAr Control

Naihao Shi, *Graduate Student Member, IEEE*, Rui Cheng, *Graduate Student Member, IEEE*, Liming Liu, *Graduate Student Member, IEEE*, Zhaoyu Wang, *Senior Member, IEEE*, Qianzhi Zhang, *Member, IEEE*

**Abstract**—This paper proposes a data-driven affinely adjustable robust Volt/VAr control (AARVVC) scheme, which modulates the smart inverter reactive power in an affine function of its active power, based on the voltage sensitivities with respect to real/reactive power injections. To achieve a fast and accurate estimation of voltage sensitivities, we propose a data-driven method based on deep neural network (DNN), together with a rule-based bus-selection process using the bidirectional search method. Our method only uses the operating statuses of selected buses as inputs to DNN, thus significantly improving the training efficiency and reducing information redundancy. Finally, a distributed consensus-based solution, based on the alternating direction method of multipliers (ADMM), for the AARVVC is applied to decide the inverter’s reactive power adjustment rule with respect to its active power. Only limited information exchange is required between each local agent and the central agent to obtain the slope of the reactive power adjustment rule, and there is no need for the central agent to solve any (sub)optimization problems. Numerical results on the modified IEEE-123 bus system validate the effectiveness and superiority of the proposed data-driven AARVVC method.

**Index Terms**—Volt/VAr control, voltage sensitivities, bidirectional search method, data-driven method.

## I. INTRODUCTION

VOLT/VAr control (VVC) has always been a critical issue for power system operations. According to the standard by American National Standards Institute [1], the voltage level should be maintained within a secure range, otherwise the performance of electrical equipment might be affected. Along with the growing trend of distributed energy resources (DERs), the ability of voltage support for distribution networks also needs further improvements. According to the IEEE standard 1547-2018, proactive voltage regulations are mandatory rather than optional for power systems [2]. But considering the long reaction time and high operation cost, the legacy voltage regulation devices cannot provide dynamic voltage support in shorter time periods against the fluctuating voltage issues. Compared with switch-based legacy voltage regulation devices, power electronics-based smart inverters have a much shorter response time and better controllability [3]. They can both absorb or inject reactive power to eliminate the rapid voltage fluctuations across power systems. Authors in [4] declaim that the high penetration of DERs may bring more difficulties in coordinating different voltage regulation devices.

Naihao Shi, Rui Cheng, Liming Liu, Zhaoyu Wang and Qianzhi Zhang are with the Department of Electrical and Computer Engineering, Iowa State University, Ames, IA 50011 USA (e-mail: snh0812@iastate.edu; ruicheng@iastate.edu; limingl@iastate.edu; wzy@iastate.edu; qianzhi@iastate.edu).

In order to coordinate both the switch-based discrete devices and responsive smart inverters for voltage regulation, VVC problems in distribution networks are often formulated as optimal power flow (OPF) problems to maintain the system voltage level within a pre-defined range while accomplishing different objectives, e.g., minimizing system loss [5], reducing system cost [6] or minimizing system voltage deviations [7]. Taking full advantage of measurements, communications and control capabilities, different VVC strategies are proposed. In [8], a centralized VVC framework is proposed for day-ahead scheduling of different voltage regulation devices. To address voltage issues in different timescales caused by the stochastic and intermittent nature of DER, a robust two-stage VVC strategy is proposed in [9] to coordinate the discrete and continuous voltage regulation devices and find a robust optimal solution, which can cope with any possible realization within the uncertain DER output. However, the VVC problems in [8], [9] are solved in a centralized manner, leading to high communication costs and computational burdens. As discussed in [10], the advantages of distributed algorithms over centralized approaches in power systems include: (1) Limited information sharing, which can improve cybersecurity and protect data privacy; (2) Robustness with respect to the failure of individual agents; (3) The ability to perform parallel computations and better scalability. Distributed VVC strategies, based on the Alternating Direction Method of Multipliers (ADMM) [11] or projected Newton method, are applied to coordinate photovoltaic inverters [12], [13], and wind turbines [14], relying on the communication between neighboring buses/zones or the communication between the central agent and local agents.

In the centralized and distributed VVC strategies, the reactive power outputs of DERs highly rely on communication and coordination across distribution systems, lacking the self-regulation ability of local DERs to some extent. In order to enhance the self-regulation ability of local DERs, some local voltage control strategies are proposed to combine with the centralized and distributed VVC strategies. For instance, local voltage controls are combined with centralized/distributed VVC strategies in [15]–[17]. As one of the most common and popular local voltage control methods, droop control adjusts the reactive power outputs as a function of voltage magnitude following a given ‘Volt-Q’ piecewise linear characteristic. However, according to [18], [19], the droop control may lead to some stability or feasibility issues under certain circumstances. An automatic self-adaptive local voltage control is proposed in [20] to improve the stability and feasibility performance, where each bus agent can locally and dynami-

cally adjust its voltage droop function in accordance with time-varying system change. In some works, the smart inverter's reactive power adjustment is based on its local real-time active power rather than its voltage magnitude, which can be regarded as a 'P-Q' rule. More specifically, the smart inverter reactive power is adjusted as a function of its active power following a given/pre-defined 'P-Q' characteristic. In [21], the reactive power outputs of DERs are adjusted based on a quadratic relationship with the active power outputs. Researchers in [22] introduce a dynamic VVC strategy with several states, where the 'Volt-Q' rule and the 'P-Q' rule are applied to different operating statuses, respectively.

How to determine a 'P-Q' rule is the key to achieving good voltage regulation performances. By projecting the complex power flow relationship into linear space, the voltage deviations caused by the power injection fluctuations can be approximated rapidly [23] using voltage sensitivities. Taking advantage of voltage sensitivity analysis, different 'P-Q' control rules for voltage regulation are investigated. For example, in [24], an affine 'P-Q' rule is introduced against the voltage deviations caused by PV uncertainties, where the reactive power adjustment ratio is obtained by solving an optimization problem with voltage sensitivities as parameters. Besides, the affine 'P-Q' rule is further refined by incorporating voltage and inverter limit constraints in [25], resulting in fewer voltage violations and reactive power usages. But the 'P-Q' rules in [24], [25] are determined in a system-wise centralized manner. In [26], a network partition method is applied to divide the system into several zones, where the 'P-Q' rule for each zone is separately determined. That is, the 'P-Q' rule is determined in a zone-wise centralized manner without considering the interactions among zones. Both the system-wise and zone-wise centralized manner require a large amount of information exchanging and computational burdens. Moreover, as mentioned before, voltage sensitivities are the key parameters for performing 'P-Q' rules. In [24], the voltage sensitivities are calculated by inverting the Jacobian matrix, requiring a large amount of computation. Authors in [25] utilize the surface fitting technique [27], a non-linear regression method, to estimate voltage sensitivities, where each bus voltage sensitivity is approximately calculated based on the mapping from its local power injections to its local voltage. However, this technique does not consider the influences from other buses on the local bus voltage sensitivity. The sensitivity analysis in [26] relies on the perturb and observe method, which means to repeatedly inject a small amount of power at one node and calculate the impact on bus voltages. The perturb and observe method requires repeatedly solving the power flow.

To this end, a data-driven affinely adjustable robust Volt/VAR control (AARVVC) scheme is proposed to mitigate voltage issues against the PV uncertainty. In the first stage, the switch-based discrete devices and the base reactive power set points for PV inverters are determined with the goal of minimizing the total system power losses. In the second stage, the reactive power outputs of PV inverters are further adjusted, based on a data-driven affine 'P-Q' control rule, to reduce possible voltage fluctuations, where the 'P-Q' rule is decided in a distributed manner. The main contributions of this work are listed

as follows:

- A data-driven method, based on the deep neural network (DNN), is proposed to predict voltage sensitivities. Given the voltage magnitudes and power injections of pre-selected buses as inputs, the well-trained DNNs output the corresponding voltage sensitivity parameters, which are of great importance for determining the affine 'P-Q' rule. It greatly improves the speed of calculating voltage sensitivities while maintaining high prediction accuracy.
- To improve the training efficiency and reduce redundant information, a feature-selection process, based on the rule-based bus selection with a Bidirectional Search (BDS) process [28], is proposed. The operating statuses of each bus, including the bus active and reactive power injections and voltages, are regarded as one feature. Then the bus-selection problem can be converted into a feature-selection problem. The BDS process works from two directions for choosing the key buses: selecting the best feature while removing the worst feature until the pre-defined number of features are selected. By applying the BDS method, a subset of buses, selected by the BDS process, are combined with buses with PV installed to generate the buses selected for voltage sensitivity estimation. Only the operating statuses of those buses are applied to estimate the voltage sensitivities.
- The slope of the affine 'P-Q' rule is obtained in a distributed hierarchical manner by using the ADMM algorithm. Relying on the communication between the central agent and local buses, the distributed consensus-based AARVVC requires less information exchange than the system-wise and zone-wise centralized manners. Plus, the central agent is only required to average its received local decision variables from local buses, thus reducing the computation burden of the central agent.

The rest of the paper is organized as follows. Section II provides an overview of the proposed two-stage VVC strategy. The first-stage VVC strategy is formulated in Section III. Section IV presents the second-stage VVC strategy, including the data-driven voltage sensitivity estimation and the distributed consensus-based AARVVC. Numerical results on the modified IEEE-123 bus system are given in Section V and the paper is concluded in Section VI.

## II. TWO-STAGE VVC FRAMEWORK: OVERVIEW

The paper proposes a two-stage VVC framework. Based on the predicted information, the first stage aims to minimize the system power losses by dispatching the optimal settings of switch-based discrete devices and determining the optimal base reactive power set points for PV inverters. Considering the long reaction time of the discrete voltage control devices, the first-stage VVC has a slow-timescale. However, only relying on the forecast values, the intermittent nature of PV may cause unexpected voltage deviations. In the second stage, the PV deviation from its forecast value is considered. On the basis of its reactive power set point determined in the first stage, each PV inverter further adjusts its reactive power along with

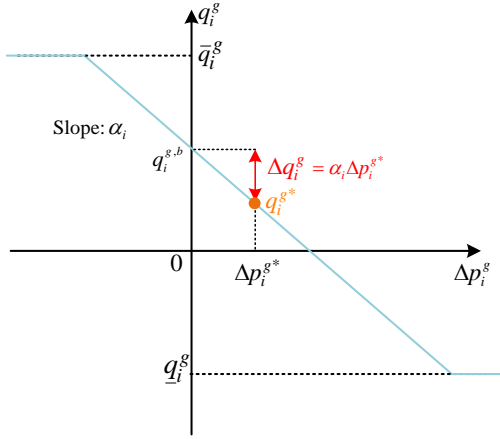


Fig. 1. The reactive power adjustment following an affine 'P-Q' rule

its real-time active power output to avoid potential voltage violations. The reactive power adjustment of PV inverter follows an optimal affine 'P-Q' rule. As shown in Fig.1,  $q_i^{g,b}$  is the PV inverter's base reactive power set point determined in the first stage, and  $\Delta p_i^{g,*}$  is the PV deviation from its forecast value. Upon the optimal affine 'P-Q' rule, the PV inverters' real-time reactive power can be adjusted as follows:

$$q_i^{g*} = q_i^{g,b} + \Delta q_i^g \quad (1)$$

with

$$\Delta q_i^g = \alpha_i \Delta p_i^{g*} \quad (2)$$

where  $\alpha_i$  is the slope of the affine 'P-Q' rule.

The value of  $\alpha_i$  is determined by solving an affinely adjustable robust problem with the goal of minimizing voltage deviations caused by the PV fluctuations. Note that voltage sensitivities with respect to active/reactive power injections are the key parameters to determine the optimal affine 'P-Q' rule. Conventionally, the voltage sensitivities can be estimated by inverting the Jacobian matrix or using the perturb and observe method, which could be time-consuming. To this end, we propose a data-driven AARVVC to determine the optimal affine 'P-Q' rule in the second stage. As shown in Fig. 2, the data-driven AARVVC for the second-stage VVC consists of two steps: (1) Data-driven voltage sensitivity estimation; (2) Distributed consensus-based AARVVC.

With respect to the data-driven voltage sensitivity estimation, the DNN is utilized to predict voltage sensitivities by using the operating statuses, including the bus active and reactive power injections and voltages, as the input. The operating statuses of each bus can be regarded as one input feature for the DNN. To improve the training efficiency and reduce redundant information behind features, a rule-based bus selection with a BDS process is first utilized to select a subset of buses whose operating statuses have a more important and greater impact on the voltage sensitivity estimation. More details about the rule-based bus selection process are provided in Section IV. Then, the DNN-based voltage sensitivity estimation is performed to predict voltage sensitivities.

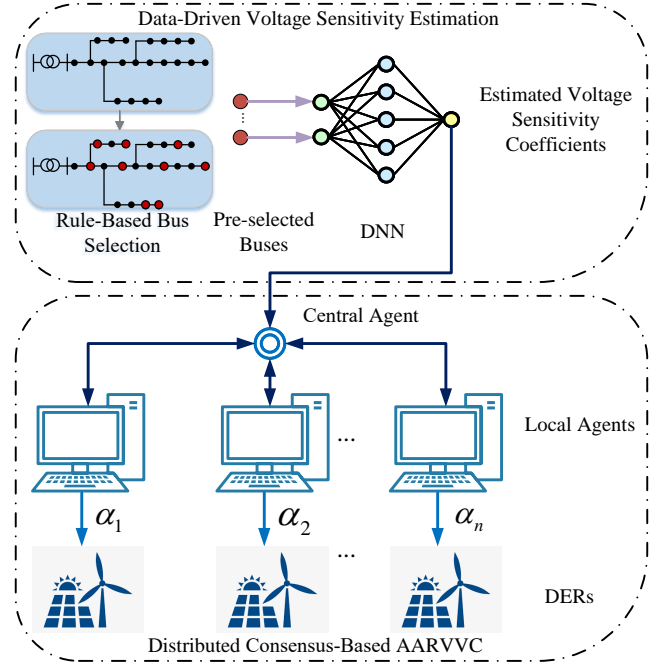


Fig. 2. The data-driven AARVVC for the second-stage VVC

Finally, a distributed consensus-based AARVVC is proposed to determine the optimal 'P-Q' rule of each PV inverter in a hierarchical manner after receiving the estimated voltage sensitivities from the DNN. The communication between the local bus agents and the central agent is required for information exchange. As every local bus agent reaches a consensus with the central agent on the optimal 'P-Q' rule, the communication process halts.

### III. FIRST-STAGE VVC STRATEGY

The first-stage VVC strategy is a deterministic OPF problem to determine the step positions of discrete devices and the optimal base reactive power set points for PV inverters based on the forecast values of DERs. The objective of this first stage is to minimize the total power losses while maintaining system voltages within the range of [0.95, 1.05].

#### A. The Distribution Network

Consider a radial distribution network containing  $n+1$  buses represented as set  $\{0\} \cup \mathcal{N}$ , where  $\{0\}$  denotes the slack bus at which the distribution network is connected to the transmission network and set  $\mathcal{N} := \{1, \dots, n\}$  denotes all other buses. Hence the radial network contains  $n$  line segments connecting the adjacent buses. For any bus  $j \in \mathcal{N}$ ,  $\mathcal{N}_j$  is the set of all children buses of bus  $j$ . The set consisting all line segments in the distribution network can be expressed as:  $\mathcal{L} = \{\ell_j = (i, j) | i = b^p(j), j \in \mathcal{N}\}$ , where  $b^p(j)$  denotes the parent bus of bus  $j$ . For each line segment  $(i, j) \in \mathcal{L}$ , let  $P_{ij}$  and  $Q_{ij}$  represent the active/reactive power flow through the line respectively,  $r_{ij}$  and  $x_{ij}$  denote the line resistance and reactance. Let  $p_i$  and  $q_i$  represent the active and reactive power injections of bus  $i$ ,  $V_i$  and  $v_i$  denote the voltage magnitude and the squared

voltage magnitude of bus  $i$ . Then the linearized distribution power flow [29], [30] can be expressed as:

$$P_{ij} = \sum_{k \in \mathcal{N}_j} P_{jk} - p_j \quad (3a)$$

$$Q_{ij} = \sum_{k \in \mathcal{N}_j} Q_{jk} - q_j \quad (3b)$$

$$v_i - v_j = 2(r_{ij}P_{ij} + x_{ij}Q_{ij}) \quad (3c)$$

### B. First-Stage VVC Problem Formulation

The active and reactive power injections of bus  $j$  are denoted by  $p_j = p_j^g - p_j^l$  and  $q_j = q_j^g - q_j^l$ , respectively. On the basis of the linearized distribution power flow, the first-stage VVC problem is formulated as:

$$\min F(t) = \sum_{(i,j) \in \mathcal{L}} r_{ij} \cdot \frac{P_{ij}^2(t) + Q_{ij}^2(t)}{v_{nom}} \quad (4)$$

subject to:

$$P_{ij}(t) = \sum_{k \in \mathcal{N}_j} P_{jk}(t) + p_j^l(t) - p_j^g(t), \forall j \in \mathcal{N} \quad (5a)$$

$$Q_{ij}(t) = \sum_{k \in \mathcal{N}_j} Q_{jk}(t) + q_j^l(t) - q_j^g(t) - q_j^c(t), \forall j \in \mathcal{N} \quad (5b)$$

$$v_i(t) - v_j(t) = 2(r_{ij}P_{ij}(t) + x_{ij}Q_{ij}(t)), \forall (i, j) \in \mathcal{L} \quad (5c)$$

$$\begin{aligned} v_0(t) &= 1 + 2n_{tap}(t)\Delta tap + (n_{tap}(t)\Delta tap)^2 \\ &\approx 1 + 2n_{tap}(t)\Delta tap \end{aligned} \quad (5d)$$

$$\underline{n}_{tap} \leq n_{tap}(t) \leq \bar{n}_{tap}, n_{tap} \in \mathbb{Z} \quad (5e)$$

$$\left| n_{tap}(t) - n_{tap}(t-1) \right| \leq \Delta n_{tap} \quad (5f)$$

$$q_i^c(t) = n_i^c(t) \cdot \Delta q_i^c, n_i^c \in \mathbb{Z} \quad (5g)$$

$$0 \leq n_i^c(t) \leq \bar{n}_i^c \quad (5h)$$

$$\left| n_i^c(t) - n_i^c(t-1) \right| \leq \Delta n_i^c \quad (5i)$$

$$-\bar{q}_i^g(t) \leq q_i^g(t) \leq \bar{q}_i^g(t), \forall i \in \mathcal{N} \quad (5j)$$

$$\bar{q}_i^g(t) = \sqrt{S_i^2 - (p_i^g(t))^2}, \forall i \in \mathcal{N} \quad (5k)$$

$$\underline{v} \leq v_i(t) \leq \bar{v}, \forall i \in \mathcal{N} \quad (5l)$$

where (4) represents the first-stage VVC goal is to minimize the total power losses. Constraints (5a)-(5c) are the linearized power flow constraints. Equation (5d) represents the voltage of the swing bus considering the on-load tap changing transformer (OLTC) where  $n_{tap}(t)$  denotes the tap position and  $\Delta tap$  denotes the tap step size. A linear approximation is applied to (5d). Equations (5e) and (5f) are the operational constraints of OLTC. The operational constraints of capacity banks and PV inverters are presented in (5g)-(5i) and (5j)-(5k), respectively. Equation (5l) is the voltage constraint. By running the first-stage VVC optimization, the optimal step positions of switch-based discrete devices and the base reactive power set points for PV inverters can be obtained.

### IV. SECOND-STAGE VVC STRATEGY: REAL-TIME ADJUSTMENT OF REACTIVE POWER

The second-stage VVC strategy focuses on the real-time adjustment for the reactive power outputs of inverters. In the first stage, the base reactive power set points for inverters are determined based on the forecast values of PV outputs without considering the uncertain characteristic of renewable energy. To avoid potential voltage issues caused by the PV fluctuations, the second-stage VVC is proposed for reactive power adjustment. A 'P-Q' affine rule is applied as the adjustment rule. The reactive power of PV inverter at bus  $i$  after the adjustment can be expressed as (6):

$$q_i^{g*} = q_i^{g,b} + \alpha_i \cdot \Delta p_i^g \quad (6)$$

Here the PV inverter reactive power  $q_i^{g*}$  can be split into two parts: the non-adjustable (or deterministic) part  $q_i^{g,b}$ , and the adjustable part which is expressed as an affine function of the PV deviation  $\Delta p_i^g$  with the slope  $\alpha_i$ . Given the slope  $\alpha_i$ , the reactive power adjustment can be calculated immediately with the real-time PV output. Therefore, the second-stage VVC strategy allows the real-time adjustment of PV inverter's reactive power in accordance with its real-time active power output to mitigate the voltage fluctuation.

### A. Second-Stage Problem Formulation: Robust Optimization Solution

The aim of the second-stage VVC strategy is to minimize the system voltage deviations due to the rapid PV fluctuations by adjusting inverters' reactive power following the optimal affine 'P-Q' rule. Let  $\mathcal{N}_G$  denote the set of all buses with PVs installed. For any bus  $i \in \mathcal{N}$ , its voltage deviation can be estimated based on voltage sensitivity:

$$\Delta V_i = \sum K_{ij}^p \cdot \Delta p_j^g + K_{ij}^q \cdot \Delta q_j^g, \forall j \in \mathcal{N}_G \quad (7)$$

where  $K_{ij}^p$  and  $K_{ij}^q$  are the voltage sensitivities at bus  $i$  to the active and reactive power injections at bus  $j$ , respectively.

It is worth mentioning that the PV deviation  $\Delta p_j^g$  from the base PV set point  $p_j^{g,b}$  is an uncertain parameter:

$$\Delta p_j^g \in [\Delta p_j^{min}, \Delta p_j^{max}], \forall j \in \mathcal{N}_G \quad (8)$$

where  $\Delta p_j^{min} \leq 0$ ,  $\Delta p_j^{max} \geq 0$  indicates that the actual PV outputs can deviate from the predicted values in both positive and negative directions. Considering the uncertain parameter  $\Delta p_j^g$ , the second-stage VVC problem can be formulated as a robust optimization problem:

$$\min \sum_{i=1}^n \left| \Delta V_i \right| \quad (9)$$

subject to:

$$(7), (8)$$

To get rid of the absolute value operator in (9), an auxiliary variable  $V_i^{aux}$  is introduced, and the problem (9) can be rewritten as follows:

$$\min \sum_{i=1}^n V_i^{aux} \quad (10)$$

subject to:

(8)

$$V_i^{aux} \geq \sum_{j=1}^n (K_{ij}^p + \alpha_j \cdot K_{ij}^q) \cdot \Delta p_j^g, \forall i \in \mathcal{N}, \forall j \in \mathcal{N}_G \quad (11a)$$

$$V_i^{aux} \geq \sum_{j=1}^n (K_{ij}^p + \alpha_j \cdot K_{ij}^q) \cdot \Delta p_j^g, \forall i \in \mathcal{N}, \forall j \in \mathcal{N}_G \quad (11b)$$

Given that  $\Delta p_i^g$  varies in the uncertainty interval, the corresponding affinely adjustable robust counterpart (AARC) [31] of (11) can be reformulated as follows:

$$\min \sum_{i=1}^n V_i^{aux} \quad (12)$$

for  $\forall i \in \mathcal{N}, \forall j \in \mathcal{N}_G$ , subject to:

$$V_i^{aux} \geq \sum_{j=1}^n (\theta'_{ij} \cdot \Delta p_j^{max} + \theta''_{ij} \cdot \Delta p_j^{min}) \quad (13a)$$

$$V_i^{aux} \geq - \sum_{j=1}^n (\theta'_{ij} \cdot \Delta p_j^{min} + \theta''_{ij} \cdot \Delta p_j^{max}) \quad (13b)$$

$$\theta'_{ij} \geq 0 \quad (13c)$$

$$\theta''_{ij} \leq 0 \quad (13d)$$

$$\theta'_{ij} \geq K_{ij}^p + \alpha_j \cdot K_{ij}^q \quad (13e)$$

$$\theta''_{ij} \leq K_{ij}^p + \alpha_j \cdot K_{ij}^q \quad (13f)$$

where  $\theta'_{ij}$  and  $\theta''_{ij}$  are the dual variables. Finally, the AARC problem reduces to a linear problem [24], whose solution is the optimal slope  $\alpha_i$  for each PV inverter.

With respect to the AARC problem, two main challenges should be considered:

(i) The first one is how to efficiently obtain the values of voltage sensitivities to the active/reactive power injections. Traditional methods to estimate voltage sensitivities, e.g., the inversion of Jacobian matrix and the perturb and observe method, can be time-consuming and complicated.

(ii) What's more is that the AARC problems (12) and (13) are formulated in a centralized manner, which means the central agent needs to collect all the information from local agents, leading to large computational burdens for the central agent.

To this end, we propose a data-driven AARVVC scheme consisting of the data-driven voltage sensitivity estimation and distributed consensus-based AARVVC.

### B. Data-Driven Voltage Sensitivity Estimation

The data-driven voltage sensitivity estimation includes the rule-based bus selection with a BDS process and the DNN-based voltage sensitivity estimation. The rule-based bus selection with a BDS process is applied to select a subset of buses whose operating statuses have a more important and greater impact on the voltage sensitivity estimation, thus improving the training efficiency and reducing redundant information. And the DNN-based voltage sensitivity estimation can efficiently predict voltage sensitivities with high accuracy.

1) *Rule-based bus selection with a BDS process:* The relationship between the voltage deviations and the deviations of bus power injections is presented as follows:

$$\begin{bmatrix} \Delta \mathbf{p} \\ \Delta \mathbf{q} \end{bmatrix} = \mathbf{J} \cdot \begin{bmatrix} \Delta \boldsymbol{\theta} \\ \Delta \mathbf{V} \end{bmatrix} \quad (14)$$

where  $\mathbf{J}$  is the Jacobian matrix,  $\Delta \mathbf{p}$  and  $\Delta \mathbf{q}$  are the deviations of bus power injections,  $\Delta \mathbf{V}$  and  $\Delta \boldsymbol{\theta}$  represent the deviations of voltage magnitudes and angles. This work mainly focuses on the impact of bus power injections on voltage magnitudes. By inverting the Jacobian matrix, the relationship between the deviations of voltage magnitudes and the deviations of bus power injections can be written as:

$$\Delta \mathbf{v} = \begin{bmatrix} \mathbf{K}^p & \mathbf{K}^q \end{bmatrix} \cdot \begin{bmatrix} \Delta \mathbf{p} \\ \Delta \mathbf{q} \end{bmatrix} \quad (15)$$

where  $\mathbf{K}^p$  and  $\mathbf{K}^q$  in (15) are sub-matrices of  $\mathbf{J}^{-1}$ . The operation of matrix inversion can be time-consuming for large-scale systems.

The entries of  $\mathbf{K}^p$  and  $\mathbf{K}^q$  are calculated from the power flow solutions, demanding operating statuses of all buses. However, there is always redundant information behind operating statuses of all buses. Besides, incorporating operating statuses of all buses as the input of DNN makes the training efficiency of DNN slow.

To this end, a rule-based bus selection with a BDS Process is utilized to pick the key buses for voltage sensitivity estimation. Only the operating statuses of the selected buses will be used to perform voltage sensitivity estimation.

The operating statuses, including the bus active and reactive power injections and its voltage, of each bus are regarded as one feature, then the bus-selection problem can be converted into a feature-selection problem, which can be resolved by the BDS feature-selection method.

As a sequential searching strategy, BDS consists of two separate processes: a sequential forward selection (SFS) which selects the feature that contributes most to improving the estimation accuracy from the remaining feature set, and a sequential backward selection (SBS) that deletes the feature which contributes the least to improving accuracy from the remaining feature set.

The procedure of the BDS is shown in **Algorithm 1: BDS-Based Bus Selection** in detail. In step S2, from all the remaining buses, one feature that contains the most information for voltage sensitivity estimation is selected and moved to the SFS set. In step S3, one feature that contributes the least in voltage sensitivity estimation is found and deleted from the remaining buses. Note that features selected by SFS will not be deleted by SBS while features removed by SBS will not be selected by SFS. This can ensure that the two processes can converge to the same solution from two directions.

In the second-stage VVC, the PV inverter's reactive power is adjusted in accordance with its real-time active power. It indicates that the operating statuses of buses with PV installed are usually necessary for the AARVVC. From a practical point of view, to reduce the investment in measuring devices, we further define a rule to combine the key buses selected by the

---

**Algorithm 1: BDS-Based Bus Selection**


---

**S1: Initialization:** Define set  $F=\emptyset$  and set  $B=\mathcal{N}$ ,  $m=0$ , and the number of buses to be selected  $n$ .

**S2: SFS process:**

Let set  $\mathcal{I}=\{i|i \notin F \text{ and } i \in B\}$ , which contains  $k$  buses  $\{i_1, i_2, \dots, i_k\}$ .

Initialize  $i^* = i_1$ ,  $\eta^* = E(F \cup i_1)$ , where  $E$  is an indicator of estimation error. The larger  $E$  is, the larger the error is.

**for**  $i = i_1, i_2, \dots, i_k$ ,

$\eta = E(F \cup i)$ ,

**if** ( $\eta \leq \eta^*$ )

$i^* = i$

$\eta^* = \eta$

**end if**

**end for**

$F = F \cup \{i^*\}$

**S3: SBS process:**

Let set  $\mathcal{J}=\{j|j \notin F \text{ and } j \in B\}$  which contains  $l$  buses  $\{j_1, j_2, \dots, j_l\}$ .

Initialize  $j^* = j_1$ ,  $\mu^* = E(B_k - j_1)$ .

**for**  $j = j_1, j_2, \dots, j_l$ ,

$\mu = E(B_k - j)$ .

**if** ( $\mu \geq \mu^*$ )

$j^* = j$

$\mu^* = \mu$

**end if**

**end for**

$B = B - \{j^*\}$

**S4: Let**  $m = m + 1$ , **and go back to S2 until**  $m = n$ , **which means that the pre-defined number of buses have been selected and added to set**  $F$ .

---

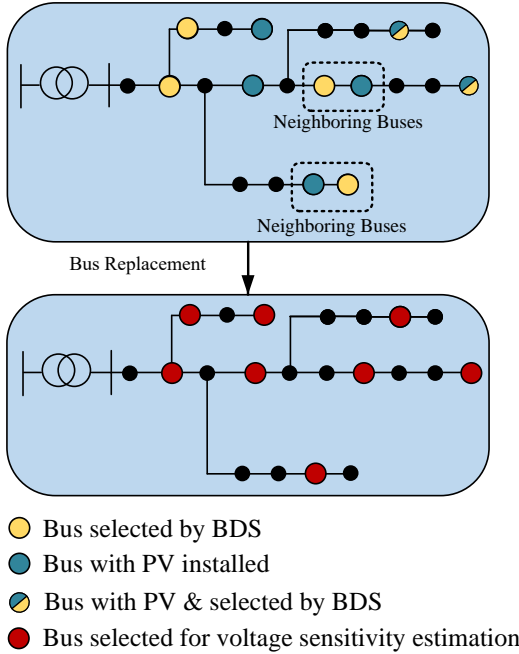


Fig. 3. Merging process of buses selected by BDS and buses with PV installed

BDS process and the buses with PV installed. The rule is defined as follows: if one bus selected by the BDS process is the neighboring bus of any bus with PV installed, then the bus, selected by the BDS process, will be replaced by its neighboring bus with PV installed. This rule is based on the intuition that there are relatively strong correlations between the operat-

ing statuses of two neighboring buses. An illustration example to explain the rule to merge buses selected by BDS and buses with PV installed is depicted in Fig.3.

2) *A DNN-based voltage sensitivity estimation:* The buses, selected by the proposed rule-based bus selection, are used for voltage sensitivity estimation. Instead of requiring the operation statuses of the whole system, only the operating statuses of selected buses are set as the input of DNN. Aiming to establish the mapping relationship from the input features to the voltage sensitivities, supervised machine learning, using a three-layer fully connected DNN, is performed. With the help of the well-trained DNN, the estimated voltage sensitivities can be obtained in real-time. Compared with the conventional methods to calculate the voltage sensitivities, the DNN-based voltage sensitivity estimation can be much more efficient and more capable of coping with the rapidly changing operating statuses of power systems.

### C. Distributed Consensus-Based AARVVC

To obtain the slope of the affine 'P-Q' rule for PV inverter in a distributed manner, we propose the distributed consensus-based AARVVC to solve the AARC problem (12)-(13). For each bus  $i \in \mathcal{N}$ , we introduce  $z_i = \{z_i^j | z_i^j = \alpha_j, \forall j \in \mathcal{N}_G\}$ , and let  $z = \{z_i | \forall i \in \mathcal{N}\}$ . Then the AARC problem (12)-(13) can be reformulated as follows:

$$\min \sum_{i=1}^n V_i^{aux} \quad (16)$$

for  $\forall i \in \mathcal{N}, \forall j \in \mathcal{N}_G$ , subject to:

$$V_i^{aux} \geq \sum_{j=1}^n (\theta'_{ij} \cdot \Delta p_j^{\max} + \theta''_{ij} \cdot \Delta p_j^{\min}) \quad (17a)$$

$$V_i^{aux} \geq - \sum_{j=1}^n (\theta'_{ij} \cdot \Delta p_j^{\min} + \theta''_{ij} \cdot \Delta p_j^{\max}) \quad (17b)$$

$$\theta'_{ij} \geq 0 \quad (17c)$$

$$\theta''_{ij} \leq 0 \quad (17d)$$

$$\theta'_{ij} \geq K_{ij}^p + z_i^j * K_{ij}^q \quad (17e)$$

$$\theta''_{ij} \leq K_{ij}^p + z_i^j * K_{ij}^q \quad (17f)$$

$$z_i^j = \alpha_j \quad (17g)$$

Note  $\Delta p^{\min} = [\Delta p_j^{\min}]_{j \in \mathcal{N}_G}$ ,  $\Delta p^{\max} = [\Delta p_j^{\max}]_{j \in \mathcal{N}_G}$  are the uncertain parameters, which are assumed to be accessed by each bus  $i \in \mathcal{N}$  in this paper, and  $K_{ij}^p, K_{ij}^q$  are the voltage sensitivity of bus  $i$  with respect to the active and reactive power of bus  $j$ , which can be accessed by bus  $i$ . It is worth mentioning  $K_{ij}^p, K_{ij}^q$  can be estimated by the proposed data-driven voltage sensitivity estimation.

In addition,  $\theta'_{ij}, \theta''_{ij}$  can be regarded as the variables associated with bus  $i$ . In this case, the objective function (16) as well as the constraints (17a)-(17f) can be split into subproblems related to each bus  $i \in \mathcal{N}$ . Then, the only coupling constraint is (17g).

To deal with the coupling constraint (17g), let  $\lambda = \{\lambda_i | i \in \mathcal{N}\}$ , where  $\lambda_i = \{\lambda_i^j | j \in \mathcal{N}_G\}$ , denote dual variables associ-



---

**Algorithm 2:** Distributed Consensus-Based AARVVC
 

---

**S1: Initialization.** Let the number of iterations  $k = 1$ ,  $\alpha(1) = 0$ ,  $z_i(1) = 0$ ,  $\lambda_i(1) = 0$ ,  $\rho > 0$ .

**S2: Each local bus agent  $i$  updates  $z_i(k)$  based on the voltage sensitivities  $K_{ij}^p$  and  $K_{ij}^q$ .**

$$z_i(k+1) = \arg \min_{z_i} L_\rho^{(i)}(\alpha(k+1), z_i, \lambda_i(k))$$

s.t. (17a) – (17f)

**S3: Each local agent then communicates  $z_i(k+1)$  to the central agent.**

**S4: Collecting  $z_i(k)$  from each local bus agent  $i \in \mathcal{N}$ , the central agent then updates  $\alpha(k+1)$ . Each entry  $\alpha_j(k+1)$  of  $\alpha(k+1)$  can be expressed as:**

$$\alpha_j(k+1) = \frac{\sum_{i \in \mathcal{N}} z_i^j(k+1)}{n+1}, \forall i \in \mathcal{N}, \forall j \in \mathcal{N}_G$$

The central agent then sends  $\alpha(k+1)$  back to each local bus agent  $i$ .

**S5: Each local bus agent  $i$  updates  $\lambda_i(k+1)$ :**

$$\lambda_i(k+1) = \lambda_i(k) + \rho \cdot (z_i(k+1) - \alpha(k+1)), \forall i \in \mathcal{N}$$

**S6: Let  $k = k + 1$ . If  $k > k_{max}$ , or the consensus is achieved, stop the iteration process; otherwise, go to S2, where  $k_{max}$  is the maximum number of iterations.**

---

ated with (17g), then the augmented Lagrangian function can be written as:

$$L_\rho(\alpha, z, \lambda) = \sum_{i=1}^n L_\rho^{(i)}(\alpha_i, z_i, \lambda_i)$$

$$= \sum_{i=1}^n \left[ V_i^{aux} + \sum_{j \in \mathcal{N}_G} \left( \lambda_i^j \cdot (z_i^j - \alpha_j) + \frac{\rho}{2} \cdot \|z_i^j - \alpha_j\|^2 \right) \right] \quad (18)$$

where  $\rho$  is a parameter. Based on ADMM, the problem (16)–(17) can be solved in a distributed manner, which is shown in detail in **Algorithm 2: Distributed Consensus-Based AARVVC**.

As seen in S2 and S3 of Algorithm 2, each local agent is assigned its own subproblem to obtain the optimal values of  $z_i(k)$  and then communicates  $z_i(k)$  to the central agent using the communication capacity of the inverters during the  $k$ -th iteration. Then in step S4, the consensus-based ADMM also simplifies the iteration process and the update of  $\alpha_j$  can be realized by simply averaging all entries in the  $j$ th column of  $z$ , and the values of  $\alpha_j$  are then sent back to corresponding local agents. The local agents then update the dual variable  $\lambda_i$  based on the updated  $\alpha$ ,  $z_i$  and the parameter  $\rho$  in step S5. The iteration process will stop until the consensus is achieved among all the local agents or the maximum number of iterations is reached.

## V. NUMERICAL RESULTS

In this section, the proposed data-driven AARVVC is implemented on the modified IEEE-123 bus test system to test its performance. The modified IEEE-123 bus test system with PV generators is shown in Fig. 4. The base voltage for the

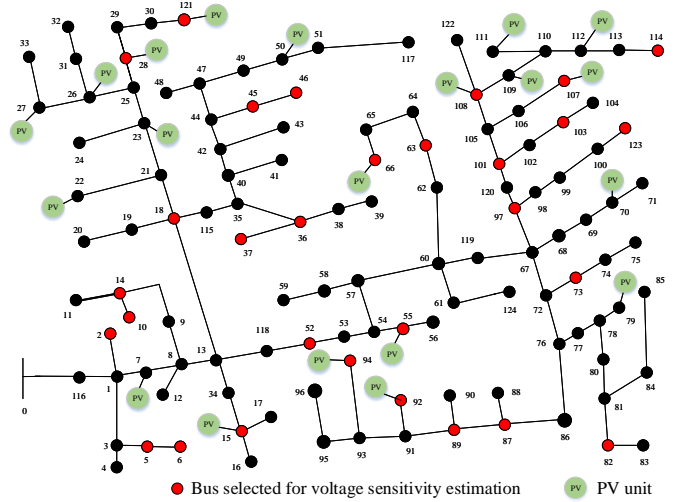


Fig. 4. The modified IEEE-123 bus test system

test system is set to 4.16 kV and the base power is set to 100 kVA. The first-stage VVC strategy is run at a circle of 15 minutes based on the forecast PV generations to dispatch the switch-based discrete devices, e.g., OLTC, and determine the base reactive power set points for PV inverters. The forecast PV penetration of this system is 47.79% in the first-stage VVC. For each single PV, a 50% uncertainty interval is considered in the second-stage VVC, indicating the uncertainty set of the PV penetration of this system can be 23.89% to 71.68%.

The step positions of discrete devices keep unchanged within the second stage. The reactive power of PV inverter is adjusted following the optimal affine ‘P-Q’ rule, determined by the proposed data-driven AARVVC. In the distributed consensus-based AARVVC, the parameter  $\rho$  is set as 0.01 and the maximum number of iterations is set as 100.

### A. Voltage Sensitivity Comparisons

As discussed before, the data-driven voltage sensitivity estimation includes two main parts: the bus-selection process and the DNN-based voltage sensitivity estimation, where the operating statuses of these selected buses are used as the input of DNN for voltage sensitivity prediction.

To evaluate the impact of the number of selected buses on the prediction accuracy, the mean average error (MAE) is chosen as the evaluation metric, which can be expressed as follows:

$$MAE = \frac{1}{n_c} \sum_{i=1}^{n_c} |x_i - \hat{x}_i| \quad (19)$$

where  $n_c$  is the number of entries of the predicted voltage sensitivities,  $x_i$  represents the real voltage sensitivity and  $\hat{x}_i$  is the estimated voltage sensitivity. The impact of the number of selected buses on MAE is depicted Fig. 5. As can be seen Fig. 5, MAE first decreases sharply as the number of selected buses increases, then MAE shows slight fluctuations as the number of selected buses is greater than 20. It shows that after the number of selected buses reaches 30, incorporating operating statuses of more buses does not contribute much to

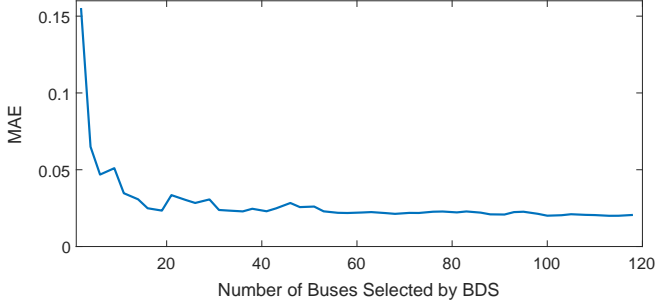


Fig. 5. MAE versus the number of selected buses.

improving the prediction accuracy of voltage sensitivity. This phenomenon indicates there is redundant information behind the operating status of all the buses.

In this case, the number of selected buses to perform voltage sensitivity estimation is set to 30. The results of the bus-selection process for the modified IEEE-123 bus test system, selected by the proposed rule-based voltage sensitivity in Section IV, are depicted as red dots in Fig.4. Those selected buses are distributed across the distribution network. It indicates information coming from almost all parts of the distribution network is incorporated in those selected buses. This might shed light on the reason why using the operating status of part of buses is enough to achieve the accurate voltage sensitivity estimation.

Taking bus 7 as an example, Fig. 6 shows the actual and estimated voltage sensitivities of each bus  $i \in \mathcal{N}$  with respect to the active and reactive power injection at bus 7, i.e.,  $dV_i/dp_7$  and  $dV_i/dq_7$  for  $\forall i \in \mathcal{N}$ . The actual voltage sensitivities are calculated by inverting the Jacobian matrix, which are regarded as the benchmark, and the estimated voltage sensitivities are calculated from the proposed data-driven voltage sensitivity estimation method. As shown in Fig. 6, the values of the estimated and actual voltage sensitivities are very close. It validates that the proposed data-driven voltage sensitivity estimation method provides accurate prediction of the voltage sensitivities by only making use of the information from the selected buses.

### B. Performance of the Distributed Consensus-Based AARVVC

As important parameters, the voltage sensitivities with respect to bus power injections, to decide the slope of the affine ‘P-Q’ rule  $\alpha_i$ , it has been validated in subsection V-A that the proposed data-driven voltage sensitivity estimation method can accurately predict voltage sensitivities. We further test the performance of our proposed Algorithm 2: Distributed Consensus-Based AAARVC.

Once the estimated voltage sensitivities are given, the slope  $\alpha_i$  of the affine ‘P-Q’ rule for each PV inverter can be determined by our proposed Algorithm 2: Distributed Consensus-Based AAARVC. Taking PV inverters at buses 7, 23, 50 and 107 as an example, the adjustment slopes for those PV inverters, determined by the distributed consensus-based AAARVC,

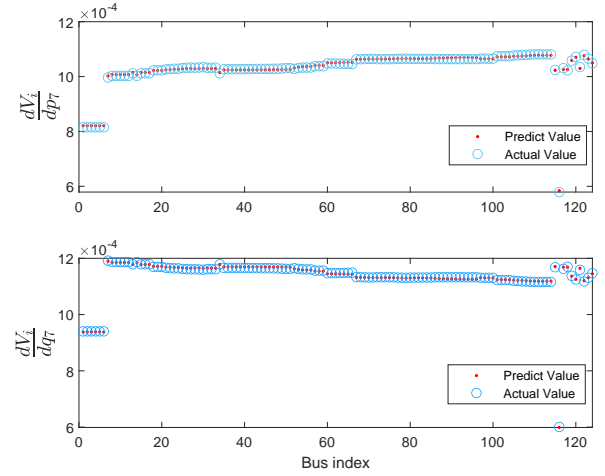


Fig. 6. Actual and estimated voltage sensitivities with respect to active and reactive power injections at bus 7

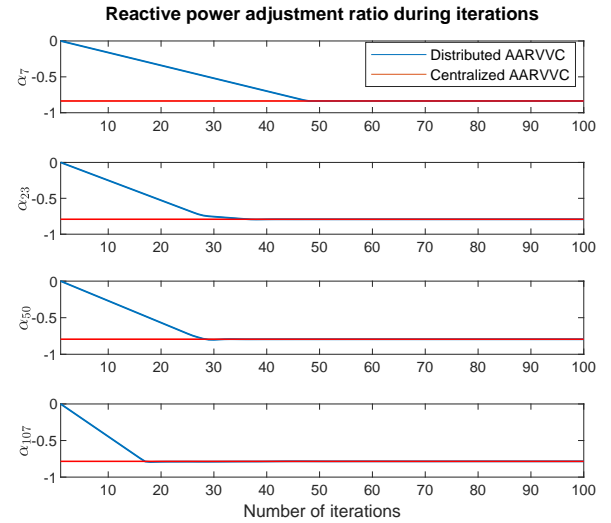


Fig. 7. Slopes for PV inverters at buses 7, 23, 50, and 107

are shown in Fig. 7. The adjustment slopes for those PV inverters solved by the centralized optimization, i.e., the AARC problem (12) and (13) is solved in a centralized manner, are depicted in Fig. 7 as the benchmark. It can be observed from Fig. 7 that all those slopes, determined by the distributed consensus-based AAARVC, can converge to the benchmark, the slopes determined by the centralized optimization. It means that the optimal ‘P-Q’ rules can be accurately calculated by our proposed distributed consensus-based AAARVC in a hierarchical distributed manner.

### C. Algorithm Comparisons

For algorithm comparisons, four different VVC schemes are considered:

Scheme 1-First-stage VVC: Only the first-stage VVC is considered.

Scheme 2-Centralized AARVVC with accurate voltage sensitivities: The AARC problem (12) and (13) is solved in a cen-



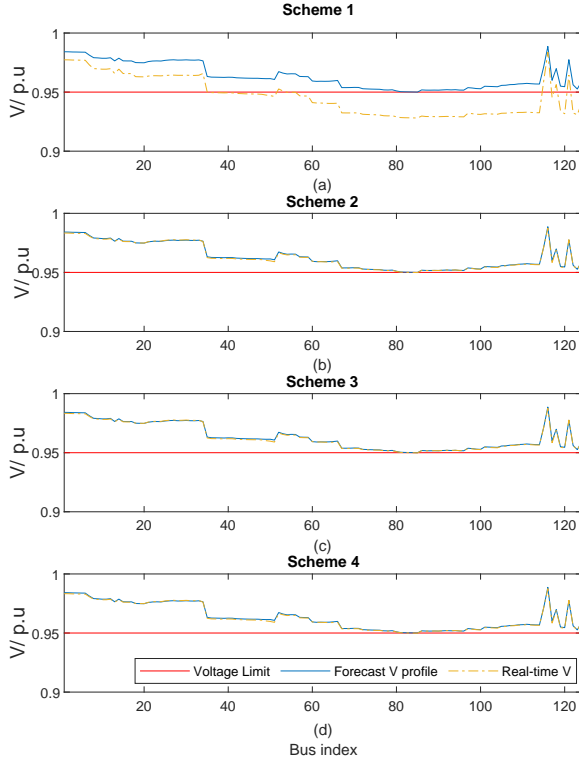


Fig. 8. The voltage profiles of different schemes under an extreme scenario

tralized manner, where the voltage sensitivities are obtained by inverting the Jacobian matrix.

**Scheme 3-Distributed consensus-based AARVVC with accurate voltage sensitives:** The AARC problem (12) and (13) is solved in a distributed consensus-based manner, where the voltage sensitivities are obtained by inverting the Jacobian matrix.

**Scheme 4-Our proposed data-driven AARVVC, i.e., distributed consensus-based AARVVC with estimated voltage sensitives:** The AARC problem (12) and (13) is solved in a distributed consensus-based manner, where the voltage sensitivities are estimated by the proposed data-driven voltage sensitivity estimation method.

Note that in Scheme 1, the reactive power outputs of PV inverters are maintained at the solution of the first-stage VVC without any adjustments. In Schemes 2-4, the reactive power outputs of PV inverters are adjusted by the determined ‘P-Q’ affine rule.

First, consider one extreme scenario, where all the PV generation is at the lowest level within the uncertainty set. The voltage profiles of the modified IEEE-123 bus test system under different schemes are presented in Fig. 8, and the number of buses with voltage violations is given in Table. I. In Fig. 8, the blue curves are the optimal voltage profiles determined in the first stage considering the forecast PV outputs, the yellow curves represent the voltage profiles in different schemes, and the red lines are voltage limits. As shown in Fig. 8, there are voltage violations for a considerable number of buses in Scheme 1. It indicates that without the second-stage reactive

power adjustment, the first-stage VVC can not maintain the voltage profiles within the acceptable range. With respect to Scheme 2 and Scheme 3, both of them utilize the accurate voltage sensitivities. The only difference between Scheme 2 and Scheme 3 is the implementation manner, where Scheme 2 is centralized and Scheme 3 is distributed. The outcomes for Scheme 2 and Scheme 3 are virtually identical, it validates our proposed distributed consensus-based AARVVC can converge to the optimal solution solved by the centralized optimization, but it is more scalable and practical. As shown in Table. I, there is only one bus with voltage violations for Scheme 1 and 2, where the lowest bus voltage magnitude for Scheme 2 and Scheme 3 is 0.949 p.u., which is very close to 0.95. For Scheme 4, its outcomes are very close to Scheme 2 and Scheme 3. The only minor difference is the number of buses with voltage violations is 2 for Scheme 4, slightly larger than Schemes 2 and 3. Such a minor difference might be caused by the error between the accurate and estimated voltage sensitives. The extreme scenario shows that the proposed data-driven AARVVC can achieve a great performance in terms of voltage regulation. To further explore the perfor-

TABLE I  
NUMBER OF BUSES WITH VOLTAGE VIOLATIONS

Scheme	1	2	3	4
Bus with Voltage Violations	75	1	1	2
Lowest Voltage (p.u.)	0.929	0.949	0.949	0.949

mance of our proposed data-driven AARVVC for voltage regulation, a Monte-Carlo simulation is carried out to randomly generate 1500 scenarios, where the PV active power output is uniformly sampled from its respective uncertainty interval. The distributions of bus voltage magnitudes under different control schemes are presented in Fig. 9. As can be seen in Fig. 9, under Scheme 1, voltages can not be maintained within the pre-defined range and the lowest voltage can be lower than 0.94. For other 3 schemes, voltages can always be maintained within the acceptable level in most scenarios. Table. II provides the ratios of bus voltage violation under different schemes. Without the second-stage VVC, 7.73 % buses are operated under voltage violations while the proposed data-driven AARVVC method can greatly decrease the ratio to around 0.5%, which is very close to the optimal performance of Scheme 2 and Scheme 3. The lowest voltage for Scheme 4 is slightly lower than 0.95 p.u.. Note that Scheme 3 is also based on our proposed distributed consensus-based AARVVC. Scheme 3 and Scheme 4 are more scalable and require fewer computation burdens compared to Scheme 2. Even though the performance of Scheme 4 is slightly inferior to Scheme 3, it is more computationally efficient as it intelligently relies on the DNN to predict voltage sensitivities.

## VI. CONCLUSION

This paper introduces a data-driven AARVVC strategy for voltage regulation against PV uncertainty. The data-driven AARVVC strategy includes two parts: the data-driven voltage sensitivity estimation and the distributed consensus-based

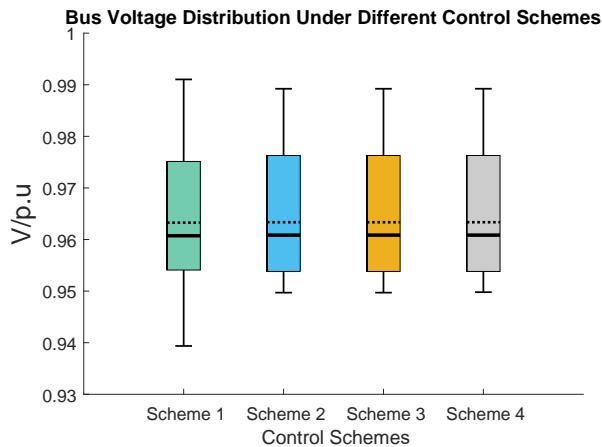


Fig. 9. Distribution of system bus voltage under different control schemes

TABLE II  
PERCENTAGE OF BUSES WITH VOLTAGE VIOLATIONS

Scheme	1	2	3	4
Bus Voltage Violation (%)	7.73	0.47	0.47	0.53
Lowest Voltage (p.u.)	0.939	0.949	0.949	0.949

AARVVC, which are performed in a distributed manner with the estimated voltage sensitivities. The voltage sensitivities are efficiently predicted by the DNN with the operating statuses of selected buses as the input. The effectiveness and superiority of the proposed data-driven AARVVC strategy are tested on the modified IEEE-123 bus test system. The results show it can accurately and efficiently estimate voltage sensitivities and achieve a good voltage regulation performance in a distributed consensus-based manner. In the future, we will take into account the network topology change.

## REFERENCES

- [1] *American National Standard for Electric Power Systems and Equipment Voltage Ratings (60 Hz)*, American National Standards Institute (ANSI) C84.1, 2016.
- [2] *IEEE Standard for Interconnection and Interoperability of Distributed Energy Resources with Associated Electric Power System Interfaces*, IEEE Std 1547-2018, 2018.
- [3] M. Farivar, R. Neal, C. Clarke, and S. Low, "Optimal inverter VAR control in distribution systems with high PV penetration," in *Proc. IEEE Power Energy Soc. General Meeting*, 2012, pp.1-7.
- [4] H. Sun, Q. Guo, J. Qi, V. Ajjarapu, R. Bravo, J. Chow, Z. Li, R. Moghe, E. Nasr-Azadani, U. Tamrakar, G. N. Taranto, R. Tonkoski, G. Valverde, Q. Wu, and G. Yang, "Review of challenges and research opportunities for voltage control in smart grids," *IEEE Trans. Power Syst.*, vol. 34, no. 4, pp. 2790–2801, Jul, 2019.
- [5] T. Ding, S. Liu, W. Yuan, Z. Bie, and B. Zeng, "A two-stage robust reactive power optimization considering uncertain wind power integration in active distribution networks," *IEEE Trans. Sustain. Energy*, vol. 7, no. 1, pp. 301–311, Jan. 2016.
- [6] G. Qu and N. Li, "Optimal distributed feedback voltage control under limited reactive power," *IEEE Trans. Power Syst.*, vol. 35, no. 1, pp. 315–331, Jan. 2020.
- [7] N. Yorino, Y. Zoka, M. Watanabe, and T. Kurushima, "An optimal autonomous decentralized control method for voltage control devices by using a multi-agent system," *IEEE Trans. Power Syst.*, vol. 30, no. 5, pp. 2225–2233, Sep. 2015.
- [8] H. Ahmadi, J. R. Martí, and H. W. Dommel, "A framework for volt-var optimization in distribution systems," *IEEE Trans. Smart Grid*, vol. 6, no. 3, pp. 1473–1483, May. 2015.
- [9] T. Ding, S. Liu, W. Yuan, Z. Bie, and B. Zeng, "A two-stage robust reactive power optimization considering uncertain wind power integration in active distribution networks," *IEEE Trans. Sustain. Energy*, vol. 7, no. 1, pp. 301–311, Jan. 2016.
- [10] D. K. Molzahn, F. Dörfler, H. Sandberg, S. H. Low, S. Chakrabarti, R. Baldick, and J. Lavaei, "A survey of distributed optimization and control algorithms for electric power systems," *IEEE Trans. Smart Grid*, vol. 8, no. 6, pp. 2941–2962, Nov. 2017.
- [11] S. Boyd, N. Parikh, E. Chu, B. Peleato, J. Eckstein, *et al.*, "Distributed optimization and statistical learning via the alternating direction method of multipliers," *Foundations and Trends® in Machine Learning*, vol. 3, no. 1, pp. 1–122, 2011.
- [12] P. Li, C. Zhang, Z. Wu, Y. Xu, M. Hu, and Z. Dong, "Distributed adaptive robust voltage/var control with network partition in active distribution networks," *IEEE Trans. Smart Grid*, vol. 11, no. 3, pp. 2245–2256, May. 2020.
- [13] R. Cheng, Z. Wang, Y. Guo, and Q. Zhang, "Online voltage control for unbalanced distribution networks using projected newton method," *IEEE Transactions on Power Systems*, pp. 1–1, in press, 2022.
- [14] Y. Guo, H. Gao, H. Xing, Q. Wu, and Z. Lin, "Decentralized coordinated voltage control for vsc-hvdc connected wind farms based on adm," *IEEE Trans. Sustain. Energy*, vol. 10, no. 2, pp. 800–810, Apr. 2019.
- [15] Y. Wang, T. Zhao, C. Ju, Y. Xu, and P. Wang, "Two-level distributed volt/var control using aggregated pv inverters in distribution networks," *IEEE Trans. Power Del.*, vol. 35, no. 4, pp. 1844–1855, Aug. 2020.
- [16] C. Zhang, Y. Xu, Y. Wang, Z. Y. Dong, and R. Zhang, "Three-stage hierarchically-coordinated voltage/var control based on pv inverters considering distribution network voltage stability," *IEEE Trans. Sustain. Energy*, vol. 13, no. 2, pp. 868–881, Apr. 2022.
- [17] S. Maharjan, A. M. Khambadkone, and J. C.-H. Peng, "Robust constrained model predictive voltage control in active distribution networks," *IEEE Trans. Sustain. Energy*, vol. 12, no. 1, pp. 400–411, Jan. 2021.
- [18] M. Farivar, L. Chen, and S. Low, "Equilibrium and dynamics of local voltage control in distribution systems," in *52nd IEEE Conference on Decision and Control*, pp. 4329–4334, 2013.
- [19] N. Li, G. Qu, and M. Dahleh, "Real-time decentralized voltage control in distribution networks," in *2014 52nd Annual Allerton Conference on Communication, Control, and Computing (Allerton)*, pp. 582–588, 2014.
- [20] R. Cheng, N. Shi, S. Maharjan, and W. Zhaoyu, "Automatic self-adaptive local voltage control under limited reactive power," *arXiv:2206.09269*, 2022.
- [21] F. U. Nazir, B. C. Pal, and R. A. Jabr, "Distributed solution of stochastic volt/var control in radial networks," *IEEE Trans. Smart Grid*, vol. 11, no. 6, pp. 5314–5324, Nov. 2020.
- [22] A. Reza Malekpour and A. Pahwa, "A dynamic operational scheme for residential pv smart inverters," *IEEE Trans. Smart Grid*, vol. 8, no. 5, pp. 2258–2267, Sep. 2017.
- [23] F. Tamp and P. Ciuffo, "A sensitivity analysis toolkit for the simplification of mv distribution network voltage management," *IEEE Trans. Smart Grid*, vol. 5, no. 2, pp. 559–568, Mar. 2014.
- [24] R. A. Jabr, "Robust volt/var control with photovoltaics," *IEEE Trans. Power Syst.*, vol. 34, no. 3, pp. 2401–2408, May. 2019.
- [25] S. M. N. R. Abadi, A. Attarha, P. Scott, and S. Thiébaux, "Affinely adjustable robust volt/var control for distribution systems with high pv penetration," *IEEE Trans. Power Syst.*, vol. 36, no. 4, pp. 3238–3247, Jul. 2021.
- [26] F. U. Nazir, B. C. Pal, and R. A. Jabr, "Affinely adjustable robust volt/var control without centralized computations," *IEEE Trans. Power Syst.*, pp. 1–1, Mar. 2022.
- [27] Z. Zhang, L. F. Ochoa, and G. Valverde, "A novel voltage sensitivity approach for the decentralized control of dg plants," *IEEE Trans. Power Syst.*, vol. 33, no. 2, pp. 1566–1576, Mar. 2018.
- [28] H. Liu and H. Motoda, *Feature selection for knowledge discovery and data mining*, vol. 454. Springer Science & Business Media, 2012.
- [29] M. E. Baran and F. F. Wu, "Optimal capacitor placement on radial distribution systems," *IEEE Trans. Power Del.*, vol. 4, no. 1, pp. 725–734, Jan. 1989.
- [30] M. E. Baran and F. F. Wu, "Network reconfiguration in distribution systems for loss reduction and load balancing," *IEEE Power Engineering Review*, vol. 9, no. 4, pp. 101–102, 1989.
- [31] A. Ben-Tal, A. Goryashko, E. Guslitzer, and A. Nemirovski, "Adjustable robust solutions of uncertain linear programs," *Mathematical programming*, vol. 99, no. 2, pp. 351–376, 2004.